

# Thermal Reactions of Titanium Thiolates: Terminal Titanium Sulfides in C–S Bond Cleavage Reactions

Andrea V. Firth, Eva Witt, and Douglas W. Stephan\*

Department of Chemistry and Biochemistry, University of Windsor,  
Windsor, Ontario, Canada N9B 3P4

Received June 1, 1998

The thermolysis of monocyclopentadienyltitanium thiolate complexes leads to ligand redistributions and C–S bond cleavage reactions. Kinetic study of the C–S bond thermolysis reaction of  $\text{CpTi}(\text{OC}_6\text{H}_3\text{-2,6-}i\text{-Pr}_2)(\text{SBn})_2$  (**2**) to the sulfide-bridged dimer  $[\text{CpTi}(\text{OC}_6\text{H}_3\text{-2,6-}i\text{-Pr}_2)(\mu\text{-S})_2]$  (**1**) is shown to be first order in **2**, consistent with an intramolecular process proceeding via a terminal sulfide intermediate and rapid dimerization ( $k = 2.8 \times 10^{-6} \text{ s}^{-1}$ ). The related species  $\text{CpTi}(\text{OC}_6\text{H}_3\text{-2,6-}i\text{-Pr}_2)(\text{SBn})\text{Cl}$  (**3**),  $\text{CpTi}(\text{OC}_6\text{H}_3\text{-2,6-}i\text{-Pr}_2)(\text{SMe})_2$  (**4**), and  $\text{CpTi}(\text{OC}_6\text{H}_3\text{-2,6-}i\text{-Pr}_2)(\text{SPh})_2$  (**5**) are thermally stable, although compounds **4** and **5** undergo thermally induced ligand redistribution reactions. These redistribution reactions are thought to occur via a dimeric intermediate in which bridging thiolate ligands are exchanged between two metal centers. A dimeric intermediate is supported by the characterization of the species  $[\text{CpTi}(\text{SR})_2(\mu\text{-SR})]_2$  ( $\text{R} = \text{Et}$  (**7**),  $\text{Bn}$  (**8**)) which are dimeric in solution at low temperature and in the solid state. In contrast,  $\text{Cp}^*\text{Ti}(\text{SBn})_3$  (**9**) is monomeric. Efforts to intercept a terminal sulfide intermediate in the formation of **1** were unsuccessful, although reaction of  $\text{CpTiCl}_2\text{Me}$  with  $\text{LiSBn}$  in the presence of  $\text{PMe}_3$  gives  $[\text{CpTiCl}(\mu\text{-S})]_2[\text{PMe}_3\text{Bn}]$  (**10**) in low yield. The analogue of **2**,  $\text{Cp}^*\text{Ti}(\text{OC}_6\text{H}_3\text{-2,6-}i\text{-Pr}_2)(\text{SBn})_2$ , **12**, is thermally stable; however, thermolysis of  $\text{Cp}^*\text{TiCl}(\text{SBn})_2$  gave  $[\text{Cp}^*\text{TiCl}(\mu\text{-S})]_2$  (**13**). Ultimately, the  $\text{LiCl}$  adduct of a terminal sulfide species  $\text{Cp}^*\text{Ti}(\text{OC}_6\text{H}_3\text{-2,6-}i\text{-Pr}_2)(\mu\text{-S})(\mu\text{-Cl})\text{Li}(\text{THF})_2$  (**14**) was isolated from the reaction of  $\text{Cp}^*\text{Ti}(\text{OC}_6\text{H}_3\text{-2,6-}i\text{-Pr}_2)\text{Cl}_2$  (**11**) with  $\text{Li}_2\text{S}$ . Treatment of (**14**) with  $\text{PMe}_3$  generates the monomeric terminal sulfide complex species  $\text{Cp}^*\text{Ti}(\text{OC}_6\text{H}_3\text{-2,6-}i\text{-Pr}_2)(\text{S})(\text{PMe}_3)$  (**15**), which is unstable, slowly evolving  $\text{PMe}_3$  affording  $[\text{Cp}^*\text{Ti}(\text{OC}_6\text{H}_3\text{-2,6-}i\text{-Pr}_2)(\mu\text{-S})_2]$  (**16**). Compound **16** is also obtained directly by heating solutions of **14**. Crystallographic studies of **8**, **10**, **12**, **13**, **14**, and **16** are reported herein. The intermediacy of terminal metal sulfides in C–S processes are discussed.

## Introduction

Transition-metal sulfide aggregates are of well-documented importance in biological systems<sup>1–3</sup> and industrial processes such as dehydrosulfurization and catalysis.<sup>4</sup> Complexes containing terminal sulfide ligands are much less common, and in fact, it has only been recently that such species have been reported for group 4 metals. The anionic terminal sulfide complex  $[\text{Ti}(\text{S})\text{Cl}_4]^{2-}$  was the first such species described.<sup>5</sup> Subsequently, the research groups of Bergman<sup>6</sup> and Parkin<sup>7–9</sup> reported the synthesis and chemistry of the complexes  $\text{Cp}^*_2\text{M}(\text{S})\text{py}$  ( $\text{M} = \text{Ti}, \text{Zr}$ ). More recently,

(1) Robson, R. L.; Eady, R. R.; Richardson, T. H.; Miller, R. W.; Hawkins, M.; Postgate, J. R. *Nature* **1986**, *322*, 388.

(2) Hales, B. J.; Case, E. E.; Morningstar, J. E.; Dzeda, M. F.; Mauterer, L. A. *Biochemistry* **1986**, *25*, 7251.

(3) Kustin, K.; Macara, I. G. *Comm. Inorg. Chem.* **1982**, *2*, 1.

(4) Steifel, E. I.; Matasumoto, K. *Transition Metal Sulfur Chemistry, Biological and Industrial Significance*, American Chemical Society: Washington, DC, 1996.

(5) Muller, U.; Krug, V. *Angew. Chem., Int. Ed. Engl.* **1988**, *27*, 293.

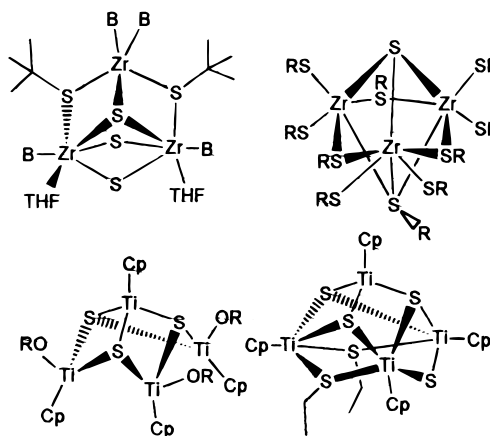
(6) Sweeney, Z. K.; Polse, J. L.; Andersen, R. A.; Bergman, R. G.; Kubinec, M. G. *J. Am. Chem. Soc.* **1997**, *119*, 4543.

(7) Howard, W. A.; Parkin, G.; Rheingold, A. *Polyhedron* **1995**, *14*, 25.

(8) Trnka, T. M.; Parkin, G. *Polyhedron* **1997**, *16*, 1031.

(9) Howard, W. A.; Trnka, T. M.; Waters, M.; Parkin, G. *J. Organomet. Chem.* **1997**, *528*, 95–121.

## Scheme 1. Early Transition Metal Sulfur Aggregates

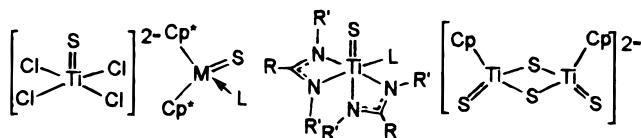


Kubas et al.<sup>10</sup> has described the dimeric species  $[\text{CpTi}(\mu\text{-S})(\text{S})]_2^{2-}$  while Hagadorn and Arnold<sup>11</sup> reported the species  $(\text{PhC}(\text{NSiMe}_3)_2)_2\text{Ti}(\text{S})\text{py}$  (Scheme 2). With the exception of the two salts, synthetic pathways to these

(10) Lundmark, P. J.; Kubas, G. L.; Scott, B. L. *Organometallics* **1996**, *15*, 3631.

(11) Hagadorn, J. R.; Arnold, J. *Inorg. Chem.* **1997**, *36*, 2928.

## Scheme 2. Group IV Metal Terminal Sulfides



terminal sulfide complexes involve oxidation of a M(II) species by sulfur. C–S bond cleavage is an alternative route to M–S bond formation. The research groups of Winter<sup>12</sup> and Bochmann<sup>13</sup> have produced TiS and TiS<sub>2</sub> films from titanium thiolate precursors. In an analogous manner, M–S aggregates as Zr<sub>3</sub>S<sub>3</sub>(*t*-BuS)<sub>2</sub>(BH<sub>4</sub>)<sub>4</sub>(THF)<sub>2</sub> and Zr<sub>6</sub>S<sub>6</sub>(*t*-BuS)<sub>4</sub>(BH<sub>4</sub>)<sub>8</sub>(THF)<sub>2</sub>,<sup>14</sup> Zr<sub>3</sub>S(S-*t*-Bu)<sub>10</sub>,<sup>15</sup> (CpTi)<sub>4</sub>(μ<sup>3</sup>-S)<sub>3</sub>(μ<sup>2</sup>-S)(μ<sup>2</sup>-SEt)<sub>2</sub>, (CpTi)<sub>6</sub>(μ<sup>3</sup>-S)<sub>4</sub>(μ<sup>3</sup>-O)<sub>4</sub>,<sup>16</sup> and [(CpTi(OC<sub>6</sub>H<sub>3</sub>-2,6-*i*-Pr<sub>2</sub>)(μ<sup>3</sup>-S))<sub>3</sub>TiCp]<sup>17</sup> have been prepared via C–S bond thermolysis reactions. Some of the more recent examples are depicted in Scheme 1. More recently, we have described the high-yield thermolysis of CpTi(OC<sub>6</sub>H<sub>3</sub>-2,6-*i*-Pr<sub>2</sub>)(Sbn)<sub>2</sub> (2) to the sulfide-bridged dimer [CpTi(OC<sub>6</sub>H<sub>3</sub>-2,6-*i*-Pr<sub>2</sub>)(μ-S)]<sub>2</sub> (1).<sup>17</sup>

Unlike the complex reactions affording larger M–S aggregates, the reactions of discrete monocyclopentadienyltitanium thiolate complexes, a class of compounds that has drawn little attention, are amenable to detailed study. To that end, we address herein, the nature and thermal stability of such compounds. These species undergo thermally induced ligand redistribution reactions and C–S bond thermolyses. Kinetic study and synthetic efforts affirm that C–S bond thermolysis proceeds through terminal titanium sulfide intermediates in these cases. The implications of these results for the formation of M–S aggregates via C–S bond activation are considered.

## Experimental Section

**General Data.** All preparations were done under an atmosphere of dry, O<sub>2</sub>-free N<sub>2</sub> employing either Schlenk-line techniques or a Vacuum Atmospheres inert atmosphere glovebox. Solvents were reagent grade, distilled from the appropriate drying agents under N<sub>2</sub>, and degassed by the freeze–thaw method at least 3 times prior to use. All organic reagents were purified by conventional methods. <sup>1</sup>H and <sup>13</sup>C{<sup>1</sup>H} NMR spectra were recorded on Bruker Avance 300 and 500 MHz instruments. Trace amounts of protonated solvents were used as references, and chemical shifts are reported relative to SiMe<sub>4</sub>. Low- and high-resolution EI mass spectra were obtained employing a Kratos Profile mass spectrometer outfitted with a N<sub>2</sub> glovebag enclosure for the inlet port. Combustion analyses were performed by Galbraith Laboratories Inc., Knoxville, TN, or E + R Microanalytical Laboratory, Corona, NY. CpTiCl<sub>2</sub>Me,<sup>18</sup> [CpTi(OC<sub>6</sub>H<sub>3</sub>-2,6-*i*-Pr<sub>2</sub>)(μ-S)]<sub>2</sub> (1), CpTi(OC<sub>6</sub>H<sub>3</sub>-2,6-*i*-Pr<sub>2</sub>)(Sbn)<sub>2</sub> (2), CpTi(OC<sub>6</sub>H<sub>3</sub>-2,6-*i*-Pr<sub>2</sub>)(SEt)<sub>2</sub>, CpTi(OC<sub>6</sub>H<sub>3</sub>-2,6-*i*-Pr<sub>2</sub>)(Sbn)Cl (3), and CpTi(OC<sub>6</sub>H<sub>3</sub>-2,6-*i*-Pr<sub>2</sub>)Cl<sub>2</sub> were prepared via published methods.<sup>17</sup>

(12) Winter, C. H.; Sheridan, P. H.; Lewkebandara, T. S.; Heeg, M. J.; Proscia, J. W. *J. Am. Chem. Soc.* **1992**, *114*, 1095.

(13) Bochmann, M.; Hawkins, I.; Wilson, L. M. *J. Chem. Soc., Chem. Commun.* **1988**, 344.

(14) Coucouvanis, D.; Lester, R. K.; Kanatzidis, M. G.; Kessissoglou, D. P. *J. Am. Chem. Soc.* **1985**, *107*, 8279.

(15) Coucouvanis, D.; Hadjikyriacou, A.; Kanatzidis, M. G. *J. Chem. Soc., Chem. Commun.* **1985**, 1224.

(16) Firth, A. V.; Stephan, D. W. *Inorg. Chem.* **1997**, *36*, 1260.

(17) Firth, A. V.; Stephan, D. W. *Organometallics* **1997**, *16*, 2183.

(18) Erskine, G. J.; Hurst, G. J. B.; Weinberg, E. L.; Hunter, B. K.; McCowan, J. D. *J. Organomet. Chem.* **1984**, *267*, 265.

**Synthesis of CpTi(OC<sub>6</sub>H<sub>3</sub>-2,6-*i*-Pr<sub>2</sub>)(SR)<sub>2</sub> (R = Me (4), Ph (5)).** These compounds were prepared in a similar manner, and thus, one such preparation is presented. To CpTi(OC<sub>6</sub>H<sub>3</sub>-2,6-*i*-Pr<sub>2</sub>)Cl<sub>2</sub> (100 mg, 0.26 mmol) dissolved in 2 mL of THF was added NaSMe (35 mg, 0.51 mmol). The reaction mixture was stirred for 12 h and filtered, and the solvent was removed, affording the red solid **4** in 54% yield. **4**: <sup>1</sup>H NMR (C<sub>6</sub>D<sub>6</sub>, 25 °C) δ 1.22 (d, 12H, |J<sub>H–H</sub>| = 7 Hz), 2.99 (s, 6H), 3.57 (sept, 2H, |J<sub>H–H</sub>| = 7 Hz), 6.04 (s, 5H), 7.01 (m, 3H); <sup>13</sup>C{<sup>1</sup>H} NMR (C<sub>6</sub>D<sub>6</sub>, 25 °C) δ 12.5, 24.0, 26.7, 123.4, 123.8, 131.8, 139.4, 159.5. HRMS calcd for C<sub>19</sub>H<sub>28</sub>TiOS<sub>2</sub> 384.1061, found 384.1059. **5**: Yield 56%; <sup>1</sup>H NMR (C<sub>6</sub>D<sub>6</sub>, 25 °C) δ 1.18 (s, 12H, |J<sub>H–H</sub>| = 7 Hz), 3.61 (sept, 2H, |J<sub>H–H</sub>| = 7 Hz), 6.04 (s, 5H), 6.84 (br m, 9H), 7.70 (d, 4H, |J<sub>H–H</sub>| = 7 Hz); <sup>13</sup>C{<sup>1</sup>H} NMR (C<sub>6</sub>D<sub>6</sub>, 25 °C) δ 24.4, 26.3, 117.1, 123.9, 125.2, 127.8, 128.2, 131.1, 138.2, 143.6, 162.5. HRMS calcd for C<sub>29</sub>H<sub>32</sub>TiOS<sub>2</sub> 508.1374, found 508.1374.

**Generation of 2, 4, and CpTi(OC<sub>6</sub>H<sub>3</sub>-2,6-*i*-Pr<sub>2</sub>)(SMe)(Sbn) (6).** (i) To **4** (18 mg, 0.04 mmol) dissolved in 1 mL of C<sub>6</sub>D<sub>6</sub> was added **2** (25 mg, 0.04 mmol). The mixture was allowed to stand for 10 min. (ii) To **3** (100 mg, 0.21 mmol) dissolved in 2 mL of benzene was added NaSMe (15 mg, 0.21 mmol). The reaction mixture was stirred for 12 h and filtered, and the solvent was removed. In either case, a mixture of **2**, **4**, and **6** was obtained. **6**: <sup>1</sup>H NMR (C<sub>6</sub>D<sub>6</sub>, 25 °C) δ 7.4–6.9 (m, 8H), 6.05 (s, 5H), 4.80 (d, 2H), 3.61 (sept, 2H), 2.96 (s, 3H), 1.22 (m, 12H).

**Synthesis of [CpTi(SR)<sub>2</sub>(μ-SR)]<sub>2</sub> (R = Et (7), Bn (8)).** These compounds were prepared in a similar manner, and thus, only one representative preparation is described. To CpTiCl<sub>3</sub> (50 mg, 0.23 mmol) dissolved in 5 mL of benzene was added LiSEt (46.8 mg, 0.69 mmol). The reaction mixture was stirred for 2 h and filtered, and the solvent was removed in vacuo. The residue was extracted into hexane, filtered, and allowed to stand. Dark red crystals of **7** were obtained in 71% yield. **7**: <sup>1</sup>H NMR (C<sub>7</sub>D<sub>8</sub>, 70 °C) δ 1.30 (t, 9H, |J<sub>H–H</sub>| = 7 Hz), 3.64 (q, 6H, |J<sub>H–H</sub>| = 7 Hz), 6.13 (s, 5H); <sup>13</sup>C{<sup>1</sup>H} NMR (C<sub>7</sub>D<sub>8</sub>, 70 °C) δ 12.4, 28.9, 108.2; <sup>1</sup>H NMR (C<sub>7</sub>D<sub>8</sub>, –40 °C) δ 1.26 (d of t, 6H, |J<sub>H–H</sub>| = 13, 7 Hz), 1.37 (d of t, 12H, |J<sub>H–H</sub>| = 13, 7 Hz), 2.98 (d of q, 4H, |J<sub>H–H</sub>| = 7, 13 Hz), 3.17 (d of q, 4H, |J<sub>H–H</sub>| = 7, 13 Hz), 3.32 (d of q, 8H, |J<sub>H–H</sub>| = 7, 13 Hz), 3.37 (d of q, 8H, |J<sub>H–H</sub>| = 7, 13 Hz), 6.38 (s, 10H); <sup>13</sup>C{<sup>1</sup>H} NMR (C<sub>7</sub>D<sub>8</sub>, –40 °C) δ 21.9, 23.1, 45.6, 47.0, 118.1. HRMS calcd for C<sub>11</sub>H<sub>20</sub>TiS<sub>3</sub> 296.0207, found 296.0215. **8**: Yield 62%, <sup>1</sup>H NMR (C<sub>7</sub>D<sub>8</sub>, 60 °C) δ 4.78 (s, 6H), 5.97 (s, 5H), 7.01 (br m, 9H), 7.18 (d, 6H, |J<sub>H–H</sub>| = 7 Hz); <sup>1</sup>H NMR (C<sub>7</sub>D<sub>8</sub>, –25 °C) δ 4.03 (d, 2H, |J<sub>H–H</sub>| = 13 Hz), 4.47 (d, 2H, |J<sub>H–H</sub>| = 13 Hz), 4.58 (d, 4H, |J<sub>H–H</sub>| = 13 Hz), 4.76 (d, 4H, |J<sub>H–H</sub>| = 13 Hz), 6.05 (s, 10H), 7.1–7.2 (m, br, 18H), 7.42 (d, 8H, |J<sub>H–H</sub>| = 7 Hz), 7.53 (d, 4H, |J<sub>H–H</sub>| = 7 Hz); <sup>13</sup>C{<sup>1</sup>H} NMR (C<sub>7</sub>D<sub>8</sub>, –25 °C) δ 50.3, 52.0, 114.8, 125.3, 126.9, 128.6, 128.7, 129.1, 130.1, 140.6, 142.9. HRMS calcd for C<sub>26</sub>H<sub>26</sub>TiS<sub>3</sub> 482.0675, found 482.0676. Anal. Calcd: C, 64.71; H, 5.43. Found: C, 64.55; H, 5.29.

**Synthesis of Cp\*Ti(Sbn)<sub>3</sub> (9).** To Cp\*TiCl<sub>3</sub> (100 mg, 0.34 mmol) suspended in 5 mL of pentane was added HSBn (128 mg, 1.04 mmol), followed by NEt<sub>3</sub> (110 mg, 1.09 mmol). The reaction mixture was stirred for 24 h, then filtered, after which the solvent was reduced to 0.5 mL. Red-orange crystals were obtained in 54% yield. <sup>1</sup>H NMR (C<sub>6</sub>D<sub>6</sub>, 25 °C) δ: 2.05 (s, 15H), 5.09 (s, 6H), 7.03 (m, 6H), 7.1 (m, 3H), 7.40 (d, 6H, |J<sub>H–H</sub>| = 7 Hz). <sup>13</sup>C{<sup>1</sup>H} NMR (C<sub>6</sub>D<sub>6</sub>, 25 °C) δ: 13.3, 43.2, 126.7, 128.5, 128.1, 128.8, 142.4. HRMS calcd for C<sub>31</sub>H<sub>36</sub>TiS<sub>3</sub> 552.1459, found 552.1455.

**Isolation of [CpTiCl(μ-S)]<sub>2</sub>[PMe<sub>3</sub>Bn] (10).** To CpTiCl<sub>2</sub>-Me (100 mg, 0.5 mmol) dissolved in 5 mL of benzene was added LiSbn (65 mg, 0.5 mmol), followed by excess PMe<sub>3</sub>. The reaction mixture was stirred for 12 h filtered, and allowed to stand several days. Dark red crystalline solid crystallized from benzene in low (<5%) yield.

**Synthesis of Cp\*Ti(OC<sub>6</sub>H<sub>3</sub>-2,6-*i*-Pr<sub>2</sub>)Cl<sub>2</sub> (11).** To Cp\*TiCl<sub>3</sub> (100 mg, 0.34 mmol) dissolved in 5 mL of benzene was added

HOC<sub>6</sub>H<sub>3</sub>-2,6-*i*-Pr<sub>2</sub> (62 μL, 0.34 mmol), followed by NEt<sub>3</sub> (46.8 μL, 0.34 mmol). The reaction mixture was stirred for 12 h and filtered, and the solvent volume was reduced to 0.5 mL. Yellow-orange crystals were obtained in 50% yield. <sup>1</sup>H NMR (C<sub>6</sub>D<sub>6</sub>, 25 °C) δ: 1.26 (d, 12H, |J<sub>H-H</sub>| = 7 Hz), 1.89 (s, 15H), 3.38 (sept, 2H, |J<sub>H-H</sub>| = 7 Hz), 7.04 (m, 3H). <sup>13</sup>C{<sup>1</sup>H} NMR (C<sub>6</sub>D<sub>6</sub>, 25 °C) δ: 12.5, 24.0, 26.7, 123.4, 123.8, 131.8, 139.4, 159.5. HRMS calcd for C<sub>22</sub>H<sub>32</sub>TiOCl<sub>2</sub> 430.1310, found 430.1298. Anal. Calcd: C, 61.27; H, 7.48. Found: C, 61.14; H, 7.28.

**Synthesis of Cp\*Ti(OC<sub>6</sub>H<sub>3</sub>-2,6-*i*-Pr<sub>2</sub>)(SBn)<sub>2</sub> (12).** To 11 (50 mg, 0.11 mmol) dissolved in 5 mL of benzene was added HSBn (26.3 μL, 0.22 mmol), followed by NEt<sub>3</sub> (31.3 μL, 0.22 mmol). The reaction mixture was stirred for 12 h and filtered, and the solvent volume was reduced to 0.5 mL. Yellow-orange crystals were obtained in 62% yield. <sup>1</sup>H NMR (C<sub>6</sub>D<sub>6</sub>, 25 °C) δ: 1.30 (d, 12H, |J<sub>H-H</sub>| = 7 Hz), 1.99 (s, 15H), 3.78 (sept, 2H, |J<sub>H-H</sub>| = 7 Hz), 4.91 (s, 4H), 7.07 (m, 9H, Ar), 7.35 (d, 4H, |J<sub>H-H</sub>| = 7 Hz). <sup>13</sup>C{<sup>1</sup>H} NMR (C<sub>6</sub>D<sub>6</sub>, 25 °C) δ: 12.8, 26.1, 30.3, 40.5, 111.0, 123.2, 124.2, 126.8, 127.0, 128.7, 129.1, 139.7, 143.0, 158.5. HRMS calcd for C<sub>36</sub>H<sub>46</sub>TiO<sub>2</sub> 606.2470, found 606.2445. Anal. Calcd: C, 71.26; H, 7.64. Found: C, 71.10; H, 7.33.

**Synthesis of [Cp\*TiCl(μ-S)]<sub>2</sub> (13).** To Cp\*TiCl<sub>3</sub> (100 mg, 0.34 mmol) dissolved in 5 mL of benzene was added HSBn (81.0 μL, 0.68 mmol), followed by NEt<sub>3</sub> (96.5 μL, 0.68 mmol). The reaction mixture was stirred for 12 h and filtered, and the reaction mixture was heated for 12–16 h. Upon cooling, dark red crystals formed and were subsequently isolated in 25% yield. <sup>1</sup>H NMR (C<sub>6</sub>D<sub>6</sub>, 25 °C) δ: 2.14 (s, 15H). <sup>13</sup>C{<sup>1</sup>H} NMR (C<sub>6</sub>D<sub>6</sub>, 25 °C) δ: 13.8, 131.9. HRMS calcd for C<sub>20</sub>H<sub>30</sub>Ti<sub>2</sub>S<sub>2</sub>Cl<sub>2</sub> 500.0125, found 500.0120. Anal. Calcd: C, 47.92; H, 6.03. Found: C, 47.79; H, 5.99.

**Synthesis of Cp\*Ti(OC<sub>6</sub>H<sub>3</sub>-2,6-*i*-Pr<sub>2</sub>)(μ-S)(μ-Cl)Li(THF)<sub>2</sub> (14).** To a solution of Cp\*Ti(OC<sub>6</sub>H<sub>3</sub>-2,6-*i*-Pr<sub>2</sub>)Cl<sub>2</sub> (100 mg, 0.22 mmol) dissolved in 5 mL of THF was added Li<sub>2</sub>S (11.7 mg, 0.3 mmol). The reaction mixture was stirred for 12 h and filtered, and the solvent was reduced to 0.5 mL. Yellow-orange crystals were obtained in 62% yield. <sup>1</sup>H NMR (C<sub>6</sub>D<sub>6</sub>, 25 °C) δ: 1.34 (m, 8H), 1.41 (d, 6H, |J<sub>H-H</sub>| = 7 Hz), 1.45 (d, br, 6H, |J<sub>H-H</sub>| = 7 Hz), 2.26 (s, 15H), 3.53 (m, 8H), 4.00 (br, 2H), 6.97 (t, 1H, |J<sub>H-H</sub>| = 7 Hz), 7.18 (d, 2H, |J<sub>H-H</sub>| = 7 Hz). <sup>13</sup>C{<sup>1</sup>H} NMR (C<sub>6</sub>D<sub>6</sub>, 25 °C) δ: 13.1, 24.6, 25.5, 25.9, 68.3, 119.8, 123.2, 123.8, 137.6, 152.4. Anal. Calcd for C<sub>30</sub>H<sub>48</sub>ClLiO<sub>3</sub>STi: C, 62.23; H, 8.36. Found: C, 62.13; H, 8.19.

**Generation of Cp\*Ti(OC<sub>6</sub>H<sub>3</sub>-2,6-*i*-Pr<sub>2</sub>)(S)(PMe<sub>3</sub>) (15).** To 14 (25 mg, 0.043 mmol) in 0.5 mL of C<sub>6</sub>D<sub>6</sub> was added PMe<sub>3</sub> (10.4 μL, 0.1 mmol). The mixture was filtered. NMR data indicated the formation of 15 in 42% NMR yield. <sup>1</sup>H NMR (C<sub>6</sub>D<sub>6</sub>, 25 °C) δ: 1.06 (d, 6H, |J<sub>H-H</sub>| = 7 Hz), 1.16 (d, 6H, |J<sub>H-H</sub>| = 7 Hz), 2.05 (s, 15H), 3.38 (sept, 2H), 7.00 (t, 1H, |J<sub>H-H</sub>| = 7 Hz), 7.25 (d, 2H, |J<sub>H-H</sub>| = 7 Hz). <sup>13</sup>C{<sup>1</sup>H} NMR (C<sub>6</sub>D<sub>6</sub>, 25 °C) δ: 13.5, 24.5, 25.0, 26.7, 121.3, 123.8, 126.8, 138.6, 161.5. <sup>31</sup>P NMR (C<sub>6</sub>D<sub>6</sub>, 25 °C) δ: -8.30.

**Synthesis of [Cp\*Ti(OC<sub>6</sub>H<sub>3</sub>-2,6-*i*-Pr<sub>2</sub>)(μ-S)]<sub>2</sub> (16).** A solution of 15 (100 mg) in toluene (2 mL) was heated for 1 h and filtered, and the solvent was reduced to 0.5 mL. Dark crystals of 16 formed in 54% yield. <sup>1</sup>H NMR (C<sub>6</sub>D<sub>6</sub>, 25 °C) δ: 1.29 (d, 6H, |J<sub>H-H</sub>| = 7 Hz), 1.60 (d, 6H, |J<sub>H-H</sub>| = 7 Hz), 2.01 (s, 15H), 3.55 (sept, 2H, |J<sub>H-H</sub>| = 7 Hz), 7.08 (t, 1H, |J<sub>H-H</sub>| = 7 Hz), 7.25 (d, 2H, |J<sub>H-H</sub>| = 7 Hz). <sup>13</sup>C{<sup>1</sup>H} NMR (C<sub>6</sub>D<sub>6</sub>, 25 °C) δ: 13.6, 24.7, 25.8, 26.5, 121.6, 124.0, 131.8, 138.6, 161.0. HRMS calcd for C<sub>44</sub>H<sub>64</sub>O<sub>2</sub>S<sub>2</sub>Ti<sub>2</sub> 784.3306, found 784.3305. Anal. Calcd C, 67.33; H, 8.22. Found: C, 67.21; H, 8.13.

**Kinetic Studies of the Thermolysis of 2.** The reactions performed at five concentrations of 2 in xylene-*d*<sub>11</sub> were maintained at 133 °C, and the ratio of 2 to 1 was monitored every 30 min over a 12–16 h period by <sup>1</sup>H NMR spectroscopy. Plots of the concentration of product versus time were prepared to ascertain the rate for each concentration, and subsequently, a plot of the rates versus concentration of 2 was obtained (Figure 1). A least-squares fit of these data afforded a rate

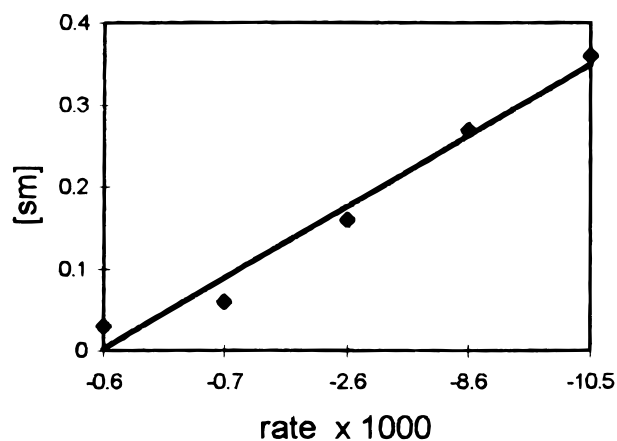


**Figure 1.** Plot of the rate of formation of 1 as a function of the concentration of 2.

constant of  $2.8 \times 10^{-6} \text{ s}^{-1}$  at 133 °C with a goodness of fit of 0.99, confirming first-order kinetics.

**X-ray Data Collection and Reduction.** X-ray quality crystals of 8, 10, 12, 13, 14, and 16 were obtained directly from the preparations as described above. The crystals were manipulated and mounted in capillaries in a glovebox, thus maintaining a dry, O<sub>2</sub>-free environment for each crystal. Diffraction experiments were performed on a Rigaku AFC6 diffractometer equipped with graphite-monochromatized Mo K $\alpha$  radiation or on a Siemens SMART system CCD diffractometer. Employing the Rigaku diffractometer, the initial orientation matrixes were obtained from 20 machine-centered reflections selected by an automated peak search routine. These data were used to determine the crystal systems. Automated Laue system check routines around each axis were consistent with the crystal system. Ultimately, 25 reflections ( $20^\circ < 2\theta < 25^\circ$ ) were used to obtain the final lattice parameters and orientation matrixes. Crystal data are summarized in Table 1. The observed extinctions were consistent with the space groups in each case. The data sets were collected in three shells ( $4.5^\circ < 2\theta < 45\text{--}50.0^\circ$ ), and three standard reflections were recorded every 197 reflections. Fixed scan rates were employed. Up to four repetitive scans of each reflection at the respective scan rates were averaged to ensure meaningful statistics. The number of scans of each reflection was determined by the intensity. The intensities of the standards showed no statistically significant change over the duration of the data collections. The data were processed using the TEXSAN crystal solution package operating on a SGI Challenger mainframe with remote X-terminals. The reflections with  $F_o^2 > 3\sigma F_o^2$  were used in the refinements.

Diffraction experiments performed on a Siemens SMART System CCD diffractometer involved collecting a hemisphere of data in 1329 frames with 10 s exposure times. A measure of decay was obtained by re-collecting the first 50 frames of each data set. The intensities of reflections within these frames showed no statistically significant change over the duration of the data collections. The data were processed using the SAINT and XPREP processing package. An empirical absorption correction based on redundant data was applied to each data set. Subsequent solution and refinement was performed using the SHELXTL solution package operating on a SGI computer.

**Structure Solution and Refinement.** Non-hydrogen atomic scattering factors were taken from the literature tabulations.<sup>19,20</sup> The Ti atom positions were determined using direct methods employing either the SHELXTL or Mithril

(19) Cromer, D. T.; Mann, J. B. *Acta Crystallogr., Sect. A* **1968**, A24, 324.

(20) Cromer, D. T.; Mann, J. B. *Acta Crystallogr., Sect. A* **1968**, A24, 390.



Table 1. Crystallographic Parameters

	<b>8</b>	<b>10</b>	<b>12</b>	<b>13</b>	<b>14</b>	<b>16</b>
formula	C <sub>32</sub> H <sub>52</sub> Ti <sub>2</sub> S <sub>6</sub>	C <sub>26</sub> H <sub>32</sub> PTi <sub>2</sub> S <sub>2</sub> Cl <sub>2</sub>	C <sub>39</sub> H <sub>49</sub> OTiS <sub>2</sub>	C <sub>30</sub> H <sub>30</sub> Ti <sub>2</sub> S <sub>2</sub> Cl <sub>2</sub>	C <sub>30</sub> H <sub>48</sub> ClLiO <sub>3</sub> STi	C <sub>44</sub> H <sub>64</sub> O <sub>2</sub> S <sub>2</sub> Ti <sub>2</sub>
fw	965.14	606.34	645.84	250.64	579.06	784.88
cryst size	0.23 × 0.19 × 0.21	0.22 × 0.22 × 0.35	0.25 × 0.24 × 0.22	0.31 × 0.24 × 0.19	0.22 × 0.20 × 0.15	0.12 × 0.26 × 0.15
<i>a</i> (Å)	13.319(4)	15.850(5)	12.226(9)	8.92(1)	11.782(5)	9.828(2)
<i>b</i> (Å)	17.232(6)	11.806(3)	15.793(3)	12.98(1)	16.300(3)	10.017(3)
<i>c</i> (Å)	11.142(3)	16.730(4)	10.028(3)	11.112(8)	9.574(6)	12.224(5)
α (deg)	102.61(3)		93.98(3)		106.82(3)	82.130(15)
β (deg)	100.13(2)	106.73(2)	103.91(3)	112.91(6)	110.54(5)	69.83(3)
γ (deg)	97.82(3)		86.06(4)		84.39(3)	71.45(2)
cryst syst	triclinic	monoclinic	triclinic	monoclinic	triclinic	triclinic
space group	<i>P</i> $\bar{1}$	<i>P</i> 2 <sub>1</sub> / <i>a</i>	<i>P</i> $\bar{1}$	<i>C</i> 2/ <i>m</i>	<i>P</i> $\bar{1}$	<i>P</i> $\bar{1}$
vol (Å <sup>3</sup> )	2415(1)	2997(1)	1872(1)	1184(2)	1648(1)	1070.4(6)
<i>D</i> <sub>calcd</sub> (g cm <sup>-3</sup> )	1.32	1.34	1.15	1.40	1.17	1.22
<i>Z</i>	2	4	2	2	2	2
abs coeff, μ, cm <sup>-1</sup>	6.24	9.16	3.67	10.78	4.30	5.04
no. of data collected	8504	5577	6598	1180	5801	5015
no. of data <i>F</i> <sub>o</sub> <sup>2</sup> > 3σ( <i>F</i> <sub>o</sub> <sup>2</sup> )	2551	787	2471	714	1412	3220
no. of variables	281	130	373	66	217	226
trans. factors	0.9248–1.0000	0.9010–1.000	na	0.738–1.000	0.745–1.000	0.290–1.000
<i>R</i> (%)	7.6	9.1	8.4	5.5	7.3	8.2
<i>R</i> <sub>w</sub> (%) <sup>a</sup>	5.1	7.9	7.5	4.5	8.6	13.9*
goodness of fit	2.00	2.15	2.37	2.45	2.20	0.75

<sup>a</sup> Weighted *R* based on all data.

direct-methods routines. The remaining non-hydrogen atoms were located from successive difference Fourier map calculations. The refinements were carried out by using full-matrix least-squares techniques on *F*, minimizing the function  $\omega(|F_o| - |F_c|)^2$  where the weight  $\omega$  is defined as  $4F_o^2/2\sigma(F_o^2)$  and *F*<sub>o</sub> and *F*<sub>c</sub> are the observed and calculated structure factor amplitudes. In the final cycles of each refinement, the number of non-hydrogen atoms assigned anisotropic temperature factors was determined so as to maintain a reasonable data:variable ratio. The remaining atoms were assigned isotropic temperature factors. Empirical absorption corrections were applied to the data sets based on either  $\psi$ -scan data or a DIFABS calculation and employing the software resident in the TEXSAN or SHELXTL packages. Hydrogen atom positions were calculated and allowed to ride on the carbon to which they are bonded, assuming a C–H bond length of 0.95 Å. Hydrogen atom temperature factors were fixed at 1.10 times the isotropic temperature factor of the carbon atom to which they are bonded. The hydrogen atom contributions were calculated but not refined. The final values of *R*, *R*<sub>w</sub>, and the goodness of fit in the final cycles of the refinements are given in Table 1. The locations of the largest peaks in the final difference Fourier map calculation as well as the magnitude of the residual electron densities in each case were of no chemical significance. Tables of crystallographic data have been deposited as Supporting Information.

## Results and Discussion

We have previously described the thermolysis of CpTi(OC<sub>6</sub>H<sub>3</sub>-2,6-*i*-Pr<sub>2</sub>)(SBn)<sub>2</sub> (**2**) to the sulfide-bridged dimer [CpTi(OC<sub>6</sub>H<sub>3</sub>-2,6-*i*-Pr<sub>2</sub>)(μ-S)]<sub>2</sub> (**1**) with the concurrent formation of SBn<sub>2</sub>.<sup>17</sup> Possible mechanisms considered for this thermolysis include inter- and intramolecular processes (Scheme 3). A bimetallic process could involve dimerization where ligand proximity prompts benzyl group transfer and elimination of dialkylsulfide. An alternative mechanism involves a unimolecular process in which benzyl group transfer to an adjacent thiolate ligand is the rate-determining step. This latter mechanism infers a terminal sulfide (Ti=S) intermediate which rapidly dimerizes. The later proposition of a terminal sulfide intermediate is supported, in principle, by the recent isolation of terminal titanium sulfide complexes.<sup>5–11</sup> A kinetic study of the reaction of **2** to **1**

was performed in *o*-xylene-*d*<sub>11</sub>. For each sample, the NMR tube containing the reaction was maintained at 133 °C and the ratio of **2** to **1** monitored every 30 min over a 12–16 h period. A plot of the rate of the formation of **1** as a function of the concentration of **2** affirms that the reaction is first order in **2** (Figure 1). This is consistent with a rate-determining step involving the intramolecular formation of a terminal sulfide intermediate followed by rapid dimerization. The pseudo-first-order rate constant was determined to be  $2.8 \times 10^{-6} \text{ s}^{-1}$ .

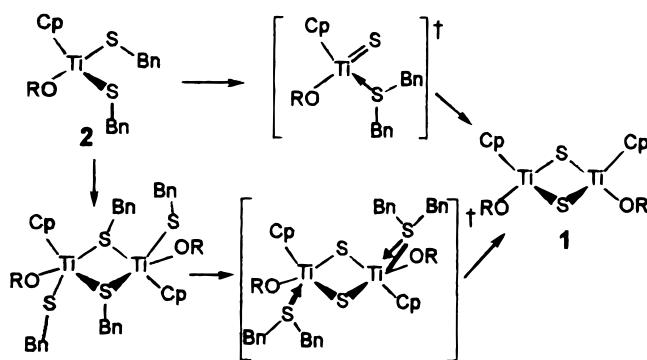
In an effort to broaden the scope of S–C bond cleavage with a view to potentially isolating an intermediate, the related species CpTi(OC<sub>6</sub>H<sub>3</sub>-2,6-*i*-Pr<sub>2</sub>)(SBn)Cl (**3**), CpTi(OC<sub>6</sub>H<sub>3</sub>-2,6-*i*-Pr<sub>2</sub>)(SMe)<sub>2</sub> (**4**), and CpTi(OC<sub>6</sub>H<sub>3</sub>-2,6-*i*-Pr<sub>2</sub>)(SPh)<sub>2</sub> (**5**) were prepared via reactions of CpTi(OC<sub>6</sub>H<sub>3</sub>-2,6-*i*-Pr<sub>2</sub>)Cl<sub>2</sub> with the appropriate thiolate. Compound **3**, like CpTi(OC<sub>6</sub>H<sub>3</sub>-2,6-*i*-Pr<sub>2</sub>)(SEt)<sub>2</sub> and CpTi(OC<sub>6</sub>H<sub>3</sub>-2,6-*i*-Pr<sub>2</sub>)(S-*t*-Bu)Cl,<sup>17</sup> was found to be thermally stable upon heating to 80 °C for 12 h, whereas compounds **4** and **5** underwent thermally induced ligand redistribution reactions. Thus, for example, heating **5** at 80 °C for a few hours resulted in the formation of a mixture containing **5**, the known species CpTi(SPh)<sub>3</sub>,<sup>21</sup> and the new, structurally characterized species CpTi(OC<sub>6</sub>H<sub>3</sub>-2,6-*i*-Pr<sub>2</sub>)<sub>2</sub>(SPh).<sup>22</sup> In a similar sense, complex **4** reacts rapidly with **2** to effect thiolate ligand scrambling, thus resulting in a statistical mixture of **2**, **4**, and CpTi(OC<sub>6</sub>H<sub>3</sub>-2,6-*i*-Pr<sub>2</sub>)(SMe)(SBn) (**6**). This same mixture of compounds is obtained in reaction of **3** and NaSMe. Spectroscopic monitoring of the thermolysis of the statistical mixture of **2**, **4**, and **6** revealed the clean formation of **1** and the sulfide byproducts SBn<sub>2</sub> and S(Bn)Me. It is clear from these results that both ligand redistribution and C–S bond cleavage reactions are markedly dependent on the electronic environment at the metal center and C–S bond strength.

Ligand redistribution reactions are thought to occur via a dimeric intermediate in which bridging thiolate

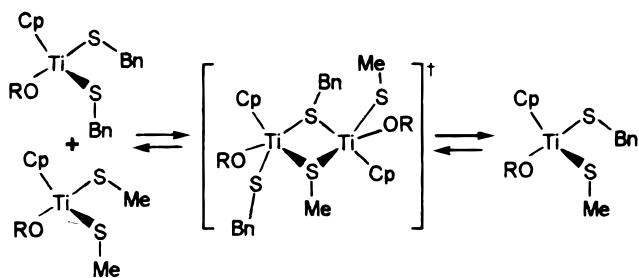
(21) Klapoetke, T.; Laskowski, R.; Kopf, H. *Z. Naturforsch., B: Chem. Sci.* **1987**, *42*, 777.

(22) Firth, A. V.; Stephan, D. W. Unpublished results.

### Scheme 3. Proposed Pathways for C–S Bond Cleavage



### Scheme 4. Proposed Mechanism for Ligand Redistribution Reactions



ligands are exchanged between the two metal centers (Scheme 4). The notion of a dimeric intermediate is conceptually supported by the structural data for the related trithiolate compound  $[\text{Cp}^*\text{Zr}(\text{SR})_2(\mu\text{-SR})_2]_2$ <sup>23</sup> as well as the thiolate-bridged titanium compound  $[\text{CpTi}(\mu^2\text{-SCH}_2\text{CH}_2\text{S})\text{Cl}]_2$ .<sup>24</sup> While these species are dynamic in solution, their dimeric nature in the solid state has been confirmed. Differing thermodynamic stabilities cannot drive analogous ligand redistribution reactions in the compounds  $[\text{CpTi}(\text{SR})_2(\mu\text{-SR})_2]$  ( $\text{R} = \text{Et}$ ,  $\text{Bn}$ ) (**8**) and  $\text{Cp}^*\text{Ti}(\text{SBn})_3$  (**9**). These species are extremely air sensitive yet are readily prepared by reaction of the respective thiol and base on  $\text{CpTiCl}_3$  or  $\text{Cp}^*\text{TiCl}_3$ . <sup>1</sup>H NMR spectra for **7** at 30 °C show broad resonances attributable to the cyclopentadienyl, methylene, and methyl protons. Upon cooling to -40 °C, these signals sharpen, giving a sharp single resonance attributable to the cyclopentadienyl protons, two triplets for the methyl groups, and three ABX<sub>3</sub> multiplets for the methylene protons. These data infer a symmetric dimeric formulation, in which two thiolate groups bridge the two metal centers. In the case of the related complex  $[\text{Cp}^*\text{Zr}(\text{SEt})_2(\mu\text{-SEt})_2]_2$ , three isomers were detected by NMR.<sup>23</sup> In contrast, only a single isomer of **7** is observed, although four structural isomers are conceivable. The NMR data infer the dominant isomer of **7** is the one in which the cyclopentadienyl and bridging thiolate ligands adopt a *transoid* disposition with respect to the  $\text{Ti}_2\text{S}_2$  core (Scheme 5). Compound **8** displays a similar temperature-dependent behavior, with three methylene resonances at -40 °C. Again, the low-temperature solution NMR data suggest a symmetric dimeric formulation for **8**. This interpretation has been confirmed crystallographically. The dissociation of **8** in

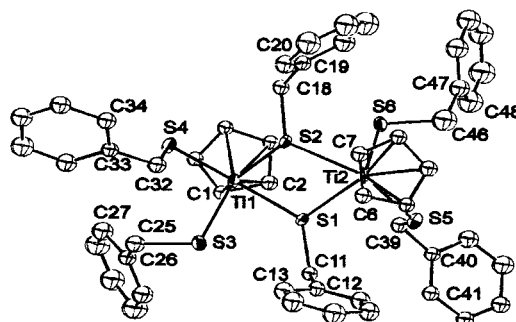
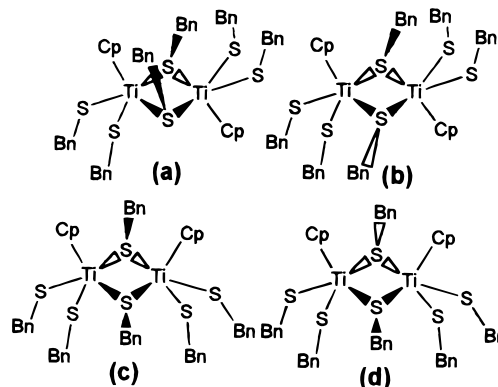


**Figure 2.** ORTEP drawing of  $[\text{CpTi}(\text{SBn})_2(\mu\text{-SBn})_2]$  (**8**); 30% thermal ellipsoids are shown.  $\text{Ti}(1)\text{-S}(1)$  2.526(4) Å;  $\text{Ti}(1)\text{-S}(2)$  2.484(4) Å;  $\text{Ti}(1)\text{-S}(3)$  2.361(4) Å;  $\text{Ti}(1)\text{-S}(4)$  2.355(4) Å;  $\text{Ti}(2)\text{-S}(1)$  2.448(4) Å;  $\text{Ti}(2)\text{-S}(2)$  2.610(4) Å;  $\text{Ti}(2)\text{-S}(5)$  2.358(4) Å;  $\text{Ti}(2)\text{-S}(6)$  2.351(4) Å;  $\text{S}(1)\text{-Ti}(1)\text{-S}(2)$  66.0(1)°;  $\text{S}(1)\text{-Ti}(1)\text{-S}(3)$  78.9(1)°;  $\text{S}(1)\text{-Ti}(1)\text{-S}(4)$  137.4(1)°;  $\text{S}(2)\text{-Ti}(1)\text{-S}(3)$  126.6(1)°;  $\text{S}(2)\text{-Ti}(1)\text{-S}(4)$  88.2(1)°;  $\text{S}(3)\text{-Ti}(1)\text{-S}(4)$  92.3(1)°;  $\text{S}(1)\text{-Ti}(2)\text{-S}(2)$  65.2(1)°;  $\text{S}(1)\text{-Ti}(2)\text{-S}(5)$  88.3(1)°;  $\text{S}(1)\text{-Ti}(2)\text{-S}(6)$  114.9(1)°;  $\text{S}(2)\text{-Ti}(2)\text{-S}(5)$  147.5(1)°;  $\text{S}(2)\text{-Ti}(2)\text{-S}(6)$  82.6(1)°;  $\text{S}(5)\text{-Ti}(2)\text{-S}(6)$  92.9(1)°;  $\text{Ti}(1)\text{-S}(1)\text{-Ti}(2)$  111.7(1)°;  $\text{Ti}(1)\text{-S}(2)\text{-Ti}(2)$  107.8(1)°.

### Scheme 5. Possible Isomers of $[\text{CpTi}(\text{SBn})_3]_2$



solution at elevated temperatures is further evidence that thermal induction of C–S bond cleavage is likely to involve a unimolecular process.

Compound **8** is a dissymmetric dimer (Figure 2) in which a thiolate ligand from each of the two  $\text{CpTi}(\text{SBn})_3$  units bridge the two metal centers. Both the cyclopentadienyl groups as well as the benzyl substituents on the bridging sulfur atoms adopt a *transoid* disposition with respect to the  $\text{Ti}_2\text{S}_2$  core. The  $\text{Ti}_2\text{S}_2$  core is not planar as the interplanar angle between the adjoining  $\text{TiS}_2$  planes is 153.5(1)°. In addition, the bridging  $\text{Ti-S}$  distances in **8** reflect a dissymmetry in the core with two longer (2.526(4), 2.610(4) Å) and two shorter distances (2.484(4), 2.448(4) Å). Within the  $\text{Ti}_2\text{S}_2$  core, the  $\text{S-Ti-S}$  angles are 111.7(1)° and 107.8(1)° at  $\text{S}(1)$  and  $\text{S}(2)$ , respectively. While the *transoid* disposition of the substituents is similar to that reported for  $[\text{Cp}^*\text{Zr}(\text{SEt})_2(\mu\text{-SEt})_2]_2$ ,<sup>23</sup> the distortions of the core is in marked contrast to the Zr analogue. The observed core distortions are attributed to steric crowding about the Ti centers.

The related complex  $\text{Cp}^*\text{Ti}(\text{SBn})_3$  (**9**) was also prepared in a manner similar to that employed for **8**; however, this species is monomeric in solution to -90 °C. The absence of association in this case is attributed to the steric demands of the pentamethylcyclopentadi-

(23) Heyn, R. H.; Stephan, D. W. *Inorg. Chem.* **1995**, *34*, 2804.

(24) Huang, Y.; Nadasdi, T. T.; Drake, R. J.; Stephan, D. W. *Inorg. Chem.* **1993**, *32*, 3022.

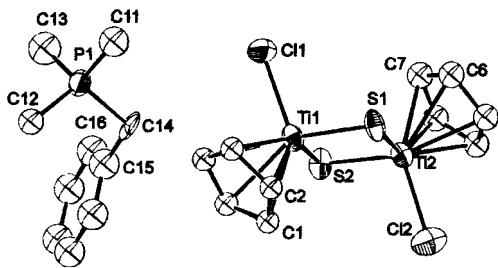


**Figure 3.** ORTEP drawing of  $[\text{CpTiCl}(\mu\text{-S})]_2[\text{PMe}_3\text{Bn}]$  (**10**); 30% thermal ellipsoids are shown. Ti(1)–Ti(2) 3.016(8) Å; Ti(1)–Cl(1) 2.35(1) Å; Ti(1)–S(1) 2.29(1) Å; Ti(1)–S(2) 2.30(1) Å; Ti(2)–Cl(2) 2.32(1) Å; Ti(2)–S(1) 2.31(1) Å; Ti(2)–S(2) 2.27(1) Å; P(1)–C(11) 1.76(4) Å; P(1)–C(12) 1.84(3) Å; P(1)–C(13) 1.74(4) Å; P(1)–C(14) 1.84(4) Å; Cl(1)–Ti(1)–S(1) 103.9(4)°; Cl(1)–Ti(1)–S(2) 102.6(4)°; S(1)–Ti(1)–S(2) 97.6(4)°; S(2)–Ti(2)–S(1) 97.9(4)°; Cl(2)–Ti(2)–S(2) 103.7(5)°; Ti(1)–S(1)–Ti(2) 81.9(4)°; Ti(1)–S(2)–Ti(2) 82.5(4)°; C(11)–P(1)–C(12) 108(2)°; C(11)–P(1)–C(13) 114(2)°; C(11)–P(1)–C(14) 106(2)°; C(12)–P(1)–C(13) 107(2)°.

enyl ligand and the resulting diminished Lewis acidity at the metal center.

The results of the kinetic study described above implicate a terminal sulfide intermediate  $\text{Cp}(\text{OR})\text{Ti}(\text{S})$  in the formation of **1**. This prompted efforts to isolate or synthesize such a sulfide derivative (or a close relative). Donor ligands such as phosphine or pyridine have recently been used to stabilize the terminal sulfide complexes, while acetylenes have been shown to undergo cycloaddition reactions with terminal chalcogenides<sup>6</sup> and phosphinidenes.<sup>25,26</sup> Thermolyses of **2** in the presence of such reagents gave rise to complex mixtures of uncharacterized products. In no case was there evidence for trapped sulfide products. However, for the reaction of  $\text{CpTiCl}_2\text{Me}$  with  $\text{LiSBn}$  in the presence of  $\text{PMe}_3$ , the crystalline product  $[\text{CpTiCl}(\mu\text{-S})]_2[\text{PMe}_3\text{Bn}]$  (**10**) was isolated in low yield. The crystallographic study of **10** (Figure 3) confirmed the formulation of this salt as formally containing a mixed-valent Ti(III)/Ti(IV) sulfide-bridged anion and the phosphonium salt cation. Structurally similar to **1**, the presence of the charge in the anion of **10** gives rise to Ti–S (2.29(1) and 2.30(1) Å), S–Ti– $S_{\text{av}}$  (97.8(3)°), and Ti–S– $Ti_{\text{av}}$  (82.2(4)°) that reflect a closer approach of the two metal centers. The resulting Ti–Ti distance in **10** (3.016(8) Å) compares with that of 3.141(3) Å seen in **1**. As **10** is formed in low yield, general conclusions regarding its mechanism of formation are not appropriate; however, it is clear that phosphine intervenes to permit transfer of a benzyl substituent to phosphorus.

In an alternative strategy to isolate a related terminal sulfide complex, the pentamethylcyclopentadienyl analogue of **1**,  $\text{Cp}^*\text{Ti}(\text{OC}_6\text{H}_3\text{-2,6-}i\text{-Pr}_2)(\text{SBn})_2$  (**12**), was also prepared in a straightforward manner via treatment of  $\text{Cp}^*\text{Ti}(\text{OC}_6\text{H}_3\text{-2,6-}i\text{-Pr}_2)\text{Cl}_2$  (**11**) with thiol and base. Spectroscopic and crystallographic data (Figure 4) confirmed the expected three-legged piano-stool geometry of compound **12**. The greater electron-donor ability of the pentamethylcyclopentadienyl ligand is reflected in the slightly longer Ti–O (**12**, 1.823(7) Å; **1**, 1.796(3) Å)<sup>9</sup> and Ti– $S_{\text{av}}$  (**12**, 2.336(4) Å; **1**, 2.329(3) Å)<sup>9</sup> bonds. The

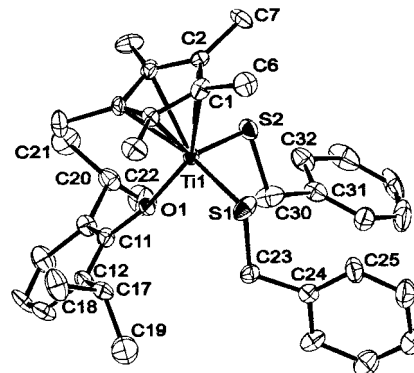


**Figure 4.** ORTEP drawing of  $\text{Cp}^*\text{Ti}(\text{OC}_6\text{H}_3\text{-2,6-}i\text{-Pr}_2)(\text{SBn})_2$  (**12**); 30% thermal ellipsoids are shown. Ti(1)–S(1) 2.342(4) Å; Ti(1)–S(2) 2.329(3) Å; Ti(1)–O(1) 1.823(7) Å; S(1)–Ti(1)–S(2) 104.9(1)°; S(1)–Ti(1)–O(1) 104.0(3)°; S(2)–Ti(1)–O(1) 103.4(2)°; Ti(1)–O(1)–C(11) 167.8(7)°; Ti(1)–S(1)–C(23) 103.5(4)°; Ti(1)–S(2)–C(30) 100.1(4)°.

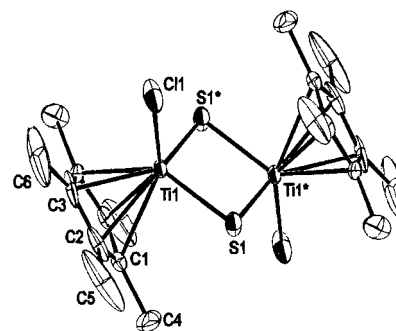


**Figure 5.** ORTEP drawing of  $[\text{Cp}^*\text{TiCl}(\mu\text{-S})]_2$  (**13**); 30% thermal ellipsoids are shown. Ti(1)–Ti(1) 3.127(3) Å; Ti(1)–Cl(1) 2.266(4) Å; Ti(1)–S(1) 2.277(2) Å; Ti(1)–S(1)' 2.277(2) Å; Cl(1)–Ti(1)–S(1) 105.00(6)°; Ti(1)–S(1)–Ti(1) 86.8(1)°; S(1)–Ti(1)–S(1)' 93.2(1)°.

Ti–O–C angle of 167.8(7)° is typical of those reported for other complexes containing the  $\text{CpTi}(\text{OR})$  fragment and is consistent with some degree of  $\pi$ -donation between O and Ti.

In contrast to **2**, compound **12** is thermally stable, even when kept at 120 °C for 18 h. This thermal stability was attributed to the enhanced electron density at Ti, although steric inhibition of the C–S bond activation could not be ruled out. In a related effort, a mixture of  $\text{Cp}^*\text{TiCl}(\text{SBn})_2$  and a lesser amount of  $\text{Cp}^*\text{TiCl}_2(\text{SBn})$  was formed in the reaction of  $\text{Cp}^*\text{TiCl}_3$  with 2 equiv of benzylthiol. While the former product is the major species, attempts to isolate this species were frustrated, presumably by ligand redistribution reactions. Nonetheless, thermolysis of this reaction mixture at 80 °C for 12 h lead to the generation of  $\text{SBn}_2$  and the sulfide-bridged dimer  $[\text{Cp}^*\text{TiCl}(\mu\text{-S})]_2$  (**13**). Formulation of **13** as a symmetric dimer is supported by the absence of the benzyl signals in the NMR data and has been confirmed by a crystallographic study (Figure 5). Two crystallographically imposed perpendicular mirror planes pass through the Ti and Cl atoms and bisect the  $\text{C}_5\text{Me}_5^-$  ligand, dictating a *transoid* disposition of the chloride and  $\text{C}_5\text{Me}_5^-$  ligands with respect to the  $\text{Ti}_2\text{S}_2$  core. The Ti–Cl distance of 2.266(4) Å is typical, while the Ti–S distance of 2.277(2) Å is shorter than that seen in **1** (2.314(4), 2.302(4) Å).<sup>17</sup> The planar  $\text{Ti}_2\text{S}_2$  core is similar in geometry to that seen in **1** with S–Ti–S and Ti–S–Ti angles of 93.2(1)° and 86.8(1)°.

(25) Breen, T. L.; Stephan, D. W. *J. Am. Chem. Soc.* **1995**, *117*, 11914.

(26) Breen, T. L.; Stephan, D. W. *J. Am. Chem. Soc.* **1996**, *118*, 4204.



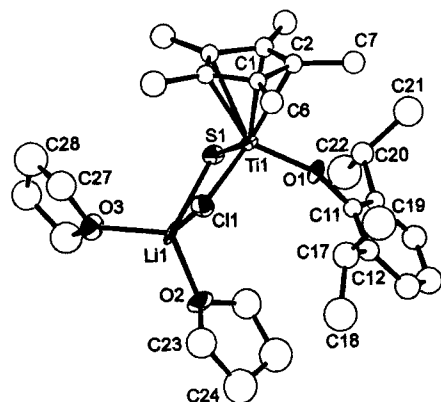
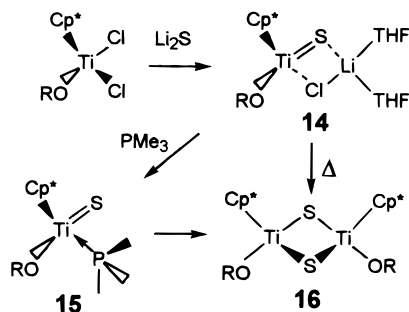


**Figure 6.** ORTEP drawing of  $\text{Cp}^*\text{Ti}(\text{OC}_6\text{H}_3\text{-2,6-}i\text{-Pr}_2)(\mu\text{-S})(\mu\text{-Cl})\text{Li}(\text{THF})_2$  (**14**); 30% thermal ellipsoids are shown. Ti(1)–Cl(1) 2.287(4) Å; Ti(1)–S(1) 2.263(4) Å; Ti(1)–O(1) 1.853(9) Å; Cl(1)–Li(1) 2.43(3) Å; S(1)–Li(1) 2.42(3) Å; O(2)–Li(1) 1.91(3) Å; O(3)–Li(1) 1.93(2) Å; Cl(1)–Ti(1)–S(1) 100.2(1)°; Cl(1)–Ti(1)–O(1) 104.4(3)°; S(1)–Ti(1)–O(1) 104.3(3)°; Ti(1)–Cl(1)–Li(1) 82.8(6)°; Ti(1)–S(1)–Li(1) 83.6(7)°; Cl(1)–Li(1)–S(1) 92(1)°.

### Scheme 6. Synthesis/Reactivity of Terminal Sulfide Adduct **14**



Although attempts to isolate or trap a terminal sulfide intermediate via C–S bond cleavage were unsuccessful, an alternative strategy has been developed which does afford a terminal sulfide derivative. Reaction of **11** with  $\text{Li}_2\text{S}$  at 25 °C yields a new orange product **14**. NMR data confirms the presence of  $\text{Cp}^*$  and aryloxy ancillary ligands as well as suggests the presence of coordinated THF. An X-ray study of **14** confirmed the formulation as  $\text{Cp}^*\text{Ti}(\text{OC}_6\text{H}_3\text{-2,6-}i\text{-Pr}_2)(\mu\text{-S})(\mu\text{-Cl})\text{Li}(\text{THF})_2$  (Figure 6). The Ti–S distance of 2.263(4) Å is somewhat longer than that seen in  $[\text{PhC}(\text{NSiMe}_3)_2]_2\text{-Ti}(\text{S})\text{Py}$  (2.139(1) Å),<sup>11</sup>  $\text{Cp}^*_2\text{Ti}(\text{S})\text{Py}$  (2.217(1) Å),<sup>6</sup>  $\text{Na}_2\text{-}[\text{CpTi}(\mu\text{-S})(\text{S})_2]$  (2.202(1), 2.187(1) Å),<sup>10</sup> and  $(\text{NET}_2)_2[\text{Ti}(\text{S})\text{Cl}_4]$  (2.111(1) Å)<sup>5</sup> but shorter than the Ti–S distances seen in **8**, **10**, and **12**. Thus, species **14** is best viewed as a LiCl adduct of the terminal sulfide fragment in which the S acts as a donor to Li and the Cl as a donor to Ti.

Treatment of **14** with  $\text{PMe}_3$  affords the species  $\text{Cp}^*\text{Ti}(\text{OC}_6\text{H}_3\text{-2,6-}i\text{-Pr}_2)(\text{S})(\text{PMe}_3)$  (**15**), Scheme 6. Spectroscopic characterization of this donor adduct of the terminal sulfide was consistent with the formulations. For example, compound **15** gives rise to a <sup>31</sup>P NMR chemical shift at –8.3 ppm, reminiscent of the shift attributed to coordinated  $\text{PMe}_3$  in  $\text{Cp}_2\text{Zr}(\text{PC}_6\text{H}_4\text{-}t\text{-Bu}_3)(\text{PMe}_3)$ .<sup>27</sup> Compound **15** is unstable, slowly evolving

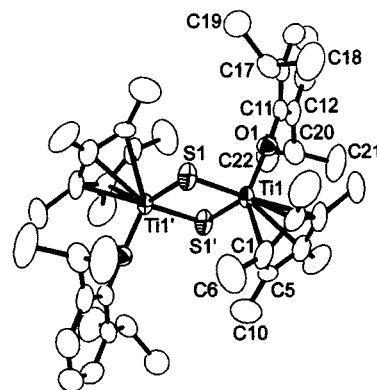


**Figure 7.** ORTEP drawing of  $[\text{Cp}^*\text{Ti}(\text{OC}_6\text{H}_3\text{-2,6-}i\text{-Pr}_2)(\mu\text{-S})_2]$  (**16**); 30% thermal ellipsoids are shown. Ti(1)–O(1) 1.827(5) Å; Ti(1)–S(1) 2.301(2) Å; Ti(1)–S(1) 2.305(3) Å; Ti(1)–Ti(1') 3.155(3) Å; S(1)–Ti(1') 2.305(3) Å; O(1)–Ti(1)–S(1) 105.1(2)°; O(1)–Ti(1)–S(1) 105.0(2)°; S(1)–Ti(1)–S(1) 93.51(9)°; Ti(1)–S(1)–Ti(1) 86.49(9)°.

$\text{PMe}_3$  at room temperature in solution and affording  $[\text{Cp}^*\text{Ti}(\text{OC}_6\text{H}_3\text{-2,6-}i\text{-Pr}_2)(\mu\text{-S})_2]$  (**16**). Compound **16** is also obtained directly by heating a solution of **14** to 80 °C for 12 h. The dimeric nature of **16** was confirmed crystallographically (Figure 7). Structural details were similar to those seen for **1** with a Ti–S distance of 2.305(3) Å and a Ti–Ti' separation of 3.155(3) Å.

The isolation of **16** from **14** is consistent with the mechanism proposed for the formation of **1**. Of course in that case the intermediate could not be intercepted. The steric bulk of the ancillary ligands in **14** and **15** has been crafted to permit isolation of the terminal sulfide. In a broader sense, these results prompt speculation regarding the possibility that larger aggregates assemble from sterically unprotected sulfide intermediates generated via similar C–S bond activation processes.

### Summary

The thermolysis of S–C bonds in **2** proceeds via a process first order in dithiolate complex, consistent with a unimolecular process and terminal-Ti–sulfide intermediate. In contrast, ligand redistribution reactions proceed via a bimolecular associative process. Attempts to intervene in C–S bond cleavage failed to access the terminal sulfide intermediate. Nonetheless, the terminal sulfide adducts are isolable employing an alternative synthetic strategy. Dimerization of these terminal sulfide species proceeds in a facile manner. While a number of other reports describe complex aggregates derived from C–S bond cleavage reactions, this report implicates monometallic terminal sulfides as intermediates in these processes. Current efforts are targeting the reactivity of terminal sulfide complexes generated in situ via C–S bond cleavage reactions as well as the use of such reactions in desulfurization chemistry.

**Acknowledgment.** Financial support from the NSERC of Canada is gratefully acknowledged. The DFG (Germany) is thanked for the award of a postdoctoral fellowship to E.W.

**Supporting Information Available:** Spectroscopic data and tables of crystallographic parameters, hydrogen atom parameters, and thermal parameters (41 pages). Ordering information is given on any current masthead page.

(27) Hou, Z.; Breen, T. L.; Stephan, D. W. *Organometallics* **1993**, *12*, 3158.